Measurement Notes

Note 51

Reduced Skin Loss Dissipation at the Edges of a Conducting Plate Using High-Voltage Rollups

J. Scott Tyo and Carl E. Baum

Phillips Laboratory/WSQ
Kirtland AFB, NM 87117

April 21, 1997

Abstract

This investigation considers a technique that mitigates dispersive skin loss effects due to enhanced currents near sharp edges in TEM transmission lines. By replacing the sharp edges with high-voltage rollups, the longitudinal currents near the edges are decreased (along with the dispersive skin losses). Approximate solutions for the current distributions on the TEM transmission line + rollup are obtained by patching together the conformal transformation corresponding to the TEM transmission line without the rollup and the conformal transformation corresponding to the high-voltage rollup at the end of a semi-infinte plate. The two current distributions are matched asymptotically to determine the appropriate transition location, thereby allowing the benefits of using high-voltage rollups near sharp edges to be determined.

I. Introduction

The dispersive effects of skin losses on the propagation of fast-rising pulses on coaxial cables have been known [1,2]. Recently, those results were extended to include the case of non-circular coaxial geometries [3,4]. For geometries with one or more knife edges, dissipation due to skin losses near the edges can be unbounded, resulting in severe degradation of the rise time of transient signals [3].

In high-voltage engineering applications, the edges of plates that serve as electrodes are sometimes rolled up to prevent electrical breakdown by reducing the magnitude of the fields at the edges of the conductors. Such a geometry was studied previously in [5], and is depicted in fig. 1. In certain applications, use of a high-voltage rollup may also be desirable in order to decrease skin losses near the edges of TEM transmission lines. In this investigation, the skin losses are examined for the cases of a plate with and without a rollup at the edge. The current is examined near the edges, and the skin losses for these two geometries are compared.

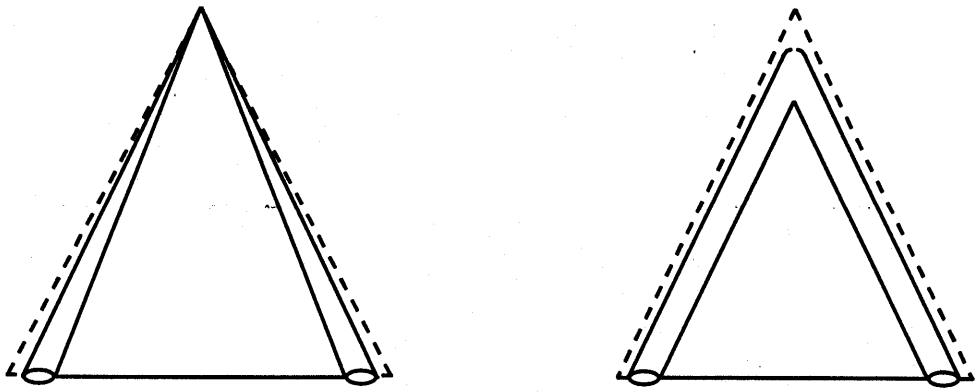

A. Conical Roll B. Cylindrical Roll

Figure 1: Two possible rollup configurations in a conical sheet.
Figure after Giri and Baum, SSN 294, figure 3

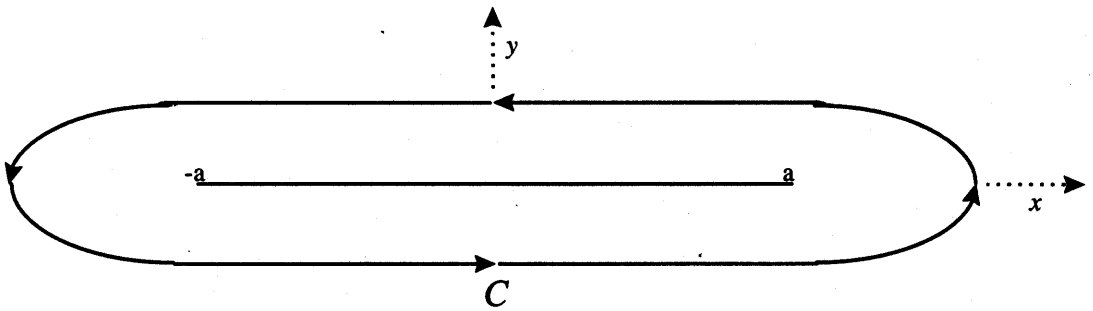

Figure 2: The isolated flat plate with the contour of integration

II. Degradation of Rise Time due to Skin Losses

For a TEM transmission line, the characteristic impedance is given as

$$\tilde{Z}' = sL' + \tilde{Z}_s' \equiv \textit{impedance per unit length (longitudinal)}$$
$$\tilde{Y}' = sC' \equiv \textit{admittance per unit length (transverse)}$$
$$\tilde{Z}_C = \left[\frac{\tilde{Z}'}{\tilde{Y}'}\right]^{1/2} = \left[\frac{sL' + \tilde{Z}_s'}{sC'}\right]^{1/2} \equiv \textit{characteristic impedance} \tag{1}$$
$$\tilde{\gamma} = \left[\tilde{Z}'\tilde{Y}'\right]^{1/2} = \left[(sL' + \tilde{Z}_s')sC'\right] \equiv \textit{propagation constant}$$

where L' is the inductance per unit length, C' is the capacitance per unit length, ~ denotes the two-sided Laplace transform over time, s is the Laplace transform variable, and

$$\tilde{Z}_s' \cong s^{\frac{1}{2}}\Xi \tag{2}$$

is an additional series impedance term due to skin losses in the non-perfect conductors. The parameter Ξ is determined by the geometry as will be seen below. For the case of $|\tilde{Z}_s'| << |sL'|$, the propagation constant can be expanded as [1,2]

$$\tilde{\gamma} = \left[(sL' + \tilde{Z}_s')sC'\right]^{1/2} = s[L'C']^{1/2} + \frac{1}{2}\frac{\tilde{Z}_s'}{Z_{C0}} + O\left(\left(\frac{\tilde{Z}_s'}{sL'}\right)^2\right); \qquad \frac{\tilde{Z}_s'}{sL'} \to 0 \tag{3}$$

where $Z_{C0} = \sqrt{\frac{L'}{C'}}$ is the characteristic impedance for perfect conductors. The cable transfer function over a distance z is given as

$$\tilde{T}(s) = \exp(-\tilde{\gamma}z) \cong \exp\left(-s[L'C']^{1/2}z\right)\exp\left(-\frac{z}{2}\frac{\tilde{Z}_s'}{Z_{C0}}\right). \tag{4}$$

The first exponential on the right side of (4) is a non-dispersive delay term, and the second exponential can be put in the form

$$-\frac{z}{2}\frac{\tilde{Z}_s'}{Z_{C0}} = [4s\tau]^{1/2}$$
$$\tau = \left[\frac{z}{4}\frac{\Xi}{Z_{C0}}\right]^2 \qquad (5)$$

The step response of the cables is given by

$$\frac{1}{s}\exp\left(-2[s\tau]^{1/2}\right) \rightarrow \operatorname{erfc}\left(\left[\frac{\tau}{t}\right]^{1/2}\right)u(t) \qquad (6)$$

where $u(t)$ is the step function and [6]

$$\operatorname{erfc}(x) = 1 - \operatorname{erf}(x)$$
$$\operatorname{erfc}(0) = 1 \qquad (7)$$
$$\operatorname{erfc}(\infty) = 0$$

It is clear from (7) that minimizing τ results in a minimization of the rise time.

For a geometry described by an arbitrary conformal transformation

$$W(\zeta) \equiv \mathrm{u}(\zeta) + jv(\zeta) \equiv \textit{complex potential}$$
$$\zeta = x + jy \equiv \textit{complex coordinate} \qquad (8)$$

the parameter Ξ is given by [3]

$$\Xi = \sum_i \left[\frac{\mu^{(i)}}{\sigma^{(i)}}\right]^{\frac{1}{2}} \mathrm{X}^{(i)}$$
$$\mathrm{X}^{(i)} = (\Delta \mathrm{v})^{-2} \oint_{C^{(i)}} \frac{1}{h_W^{(i)}} |d\mathrm{v}| \qquad (9)$$

where the summation is carried over the two conductors in the geometry with equal and opposite currents, $\mu^{(i)}$ and $\sigma^{(i)}$ are the permeability and conductivity of the i^{th} conductor, $\Delta \mathrm{v}$ is the change in v going around one of the conductors, $C^{(i)}$ is the contour around the i^{th} conductor and

$$h_W^{(i)} = \left|\frac{d\zeta}{dW}\right| \textit{on the } i^{th} \textit{ conductor}. \qquad (10)$$

III. Skin loss effects for an isolated flat plate

In this section, the risetime attributable to the skin losses on an isolated flat plate is investigated. The geometry under investigation is shown in fig. 2. The plate has width 2a, is held at a constant electric potential, and is assumed far from all other conductors. The distribution of fields (as well as longitudinal currents for a TEM transmission line) is given by the conformal transformation

$$\begin{aligned} \zeta &= a\cosh W\big|_{u=0} \\ x &= a\cos v, y = 0 \\ h_w &= \left|\frac{d\zeta}{dW}\right| = a\sqrt{\cosh^2 u - \cos^2 v} = a|\sin v| \end{aligned} \tag{11}$$

Use of (9) to determine the parameter X yields [3]

$$\begin{aligned} X &= \frac{1}{\pi^2 a} K(m=1) \\ X &\to \infty \end{aligned} \tag{12}$$

where $K(m=1)$ is the complete elliptic integral of the first kind, which diverges at $m=1$ [6]. Equation 12 implies that the rise time is unbounded for this structure. (Note, however, that the approximation of a TEM mode breaks down in this limit.)

IV. Use of a high-voltage rollup to reduce skin loss effects

The problem of diverging risetime as predicted by (12) may be alleviated by replacing the plate with sharp edges by a plate with high-voltage rollups of radius ρ. The modified geometry is depicted in fig. 3. The relative widths of the rolled-up and unrolled-up plates are chosen in fig. 3 based upon a previous study that determined the appropriate rollup size necessary to match the impedances of the structures in figs. 2 and 3 [5]. While the exact conformal transformation corresponding to the structure in fig. 3 is unknown, the field (current) distribution can be approximated (for $\rho << a$) as shown below. The value of X for the modified structure is given by

$$X = \left(\Delta v^{-2}\right) \oint_C \frac{1}{h_w(v)} dv = \frac{1}{2\pi^2} \left[\int_{C_1} \frac{1}{h_w(v)} dv + \int_{C_2} \frac{1}{h_w(v)} dv \right] \tag{13}$$

where the contour C has been split into four subcontours as shown in fig. 3. The location where the contours meet (x_0) will be determined later.

First, we attempt to approximate the integral over C_1. For $\rho << a$ and $x << a$, the fields at location x are not affected by the rollups at the ends of the plates (this assumption will constrain our choice of x_0 later) , and the field distribution is approximately given by the transformation in (11). In this case [7]

$$\int_{C_1} \frac{1}{h_w(v)} dv \cong \frac{2}{a} \int_{\arccos(x_0/a)}^{\pi/2} \frac{1}{\sin v} dv = \frac{1}{a} \ln\left(\frac{1 + x_0/a}{1 - x_0/a} \right). \tag{14}$$

The integral on C_2 can be approximated by appealing to a second conformal transformation that gives the field distribution on a semi-infinite plate with a high-voltage rollup. The transformation given by

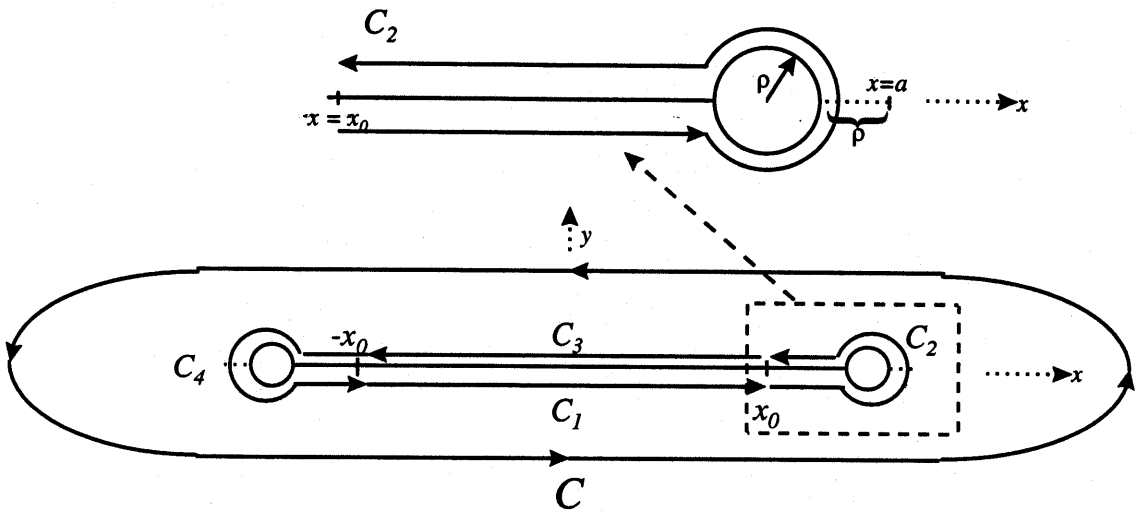

Figure 3: The modified geometry and modified contours. The dotted line indicates the additional width of a plate without rollups that would have the same impedance [5] (an extra distance ρ). The drawing at the top is a blowup of the boxed region

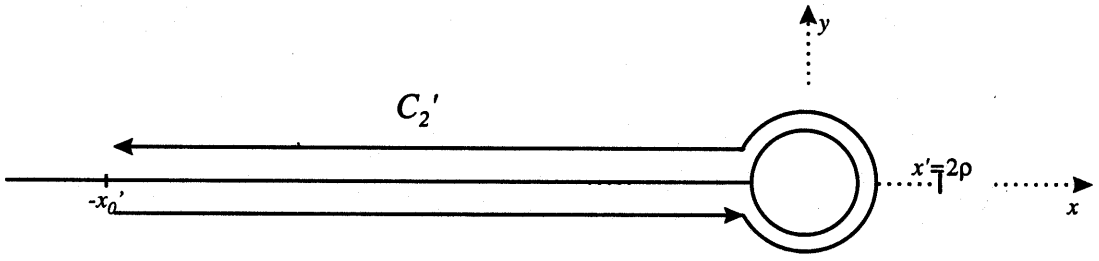

Figure 4: Semi-infinite plate with rollup and contour C_2'. The origin is assumed to be at the *center* of the rollup

$$W' = \alpha\left(\sqrt{\zeta'} - \frac{\rho}{\sqrt{\zeta'}}\right)$$

$$x' = \begin{cases} -\frac{1}{4}\left[2\left(\frac{v'}{\alpha}\right)^2 - 4\rho - 2\left|\frac{v'}{\alpha}\right|\sqrt{\left(\frac{v'}{\alpha}\right)^2 - 4\rho}\right]; & \left|\frac{v'}{\alpha}\right| > 2\sqrt{\rho} \\ \rho - \frac{(v'/\alpha)^2}{2}; & \left|\frac{v'}{\alpha}\right| < 2\sqrt{\rho} \end{cases} \qquad (15)$$

$$y' = \begin{cases} 0; & \left|\frac{v'}{\alpha}\right| > 2\sqrt{\rho} \\ \frac{(v'/\alpha)}{2}\left(4\rho - \left(\frac{v'}{\alpha}\right)^2\right); & \left|\frac{v'}{\alpha}\right| < 2\sqrt{\rho} \end{cases}$$

results in the geometry depicted in fig. 4 that has been previously described in [5]. Note that in (15), the expressions for x' and y' are solved for u′=0, which corresponds to the electrode in fig. 4. The parameter α is introduced to ensure a field match at the transition point chosen below. In order for the transformation in (15) to be appropriate, $\rho << a$ and $\rho << x_0'$ must be satisfied. The relationship between x_0 and x_0' can be inferred from figs. 3 and 4. The distance from x_0 $\left(\text{or } x_0'\right)$ to the edge of the plate (without the rollup) is equal for each case so that

$$a - x_0 = x_0' + 2\rho\,. \qquad (16)$$

For the geometry depicted in fig. 4, u' = 0 and the parameter $h_{W'}(v')$ is derived from (15) as

$$h_{W'}(v') = \left|\frac{d\zeta'}{dW'}\right| = \sqrt{\left(\frac{\partial x'}{\partial v'}\right)^2 + \left(\frac{\partial y'}{\partial v'}\right)^2}$$

$$= \begin{cases} h^{>}(v') = \frac{1}{\alpha}\left|\frac{v'}{\alpha}\right|\left[1 + \frac{1}{2}\left(1 - \frac{4\rho}{(v'/\alpha)^2}\right)^{-\frac{1}{2}} + \frac{1}{2}\left(1 - \frac{4\rho}{(v'/\alpha)^2}\right)^{\frac{1}{2}}\right], & |v'/\alpha| > 2\sqrt{\rho}\,. \\ h^{<}(v') = \frac{1}{\alpha}2\rho\left(4\rho - (v'/\alpha)^2\right)^{-\frac{1}{2}}, & |v'/\alpha| < 2\sqrt{\rho} \end{cases} \qquad (17)$$

The two regions correspond to the straight portion of the conductor and the rollup respectively. The integral over C_2 is approximated by evaluating the integral over C_2' (shown in fig. 4) as

$$\int_{C_2}\frac{1}{h_W(\mathrm{v})}d\mathrm{v}\cong\int_{C_2'}\frac{1}{h_{W'}(\mathrm{v}')}d\mathrm{v}'=\int_{-2\alpha\sqrt{\rho}}^{2\alpha\sqrt{\rho}}\frac{1}{h^{<}(\mathrm{v}')}d\mathrm{v}'+2\int_{2\alpha\sqrt{\rho}}^{\mathrm{v}'(x_0')}\frac{1}{h^{>}(\mathrm{v}')}d\mathrm{v}'=I_1+I_2. \tag{18}$$

By making the change of variables $\sigma=\mathrm{v}'/\alpha$, I_1 is evaluated as

$$I_1=\frac{\alpha^2}{2\rho}\int_{-2\sqrt{\rho}}^{2\sqrt{\rho}}\sqrt{4\rho-\sigma^2}\,d\sigma=\alpha^2\pi. \tag{19}$$

and I_2 is evaluated as

$$I_2=\int_{2\sqrt{\rho}}^{\mathrm{v}'(x_0')/\alpha}\sigma^{-1}\left[1+\tfrac{1}{2}(1-s)^{-1/2}+\tfrac{1}{2}(1-s)^{1/2}\right]^{-1}d\sigma \tag{20}$$

where $s=4\rho/\sigma^2$. The bracketed expression in (20) can be written in Taylor series form as

$$\begin{aligned}f(s)&=1+\tfrac{1}{2}(1-s)^{-1/2}+\tfrac{1}{2}(1-s)^{1/2}=2\left(1+\sum_{n=2}^{\infty}b_n s^n\right)\\ b_n&=\frac{(2n-3)!!}{2^{n-1}n!}(2n-2)\end{aligned} \tag{21}$$

with the notation

$$\begin{aligned}n!!&=n\times(n-2)\times(n-4)\times\cdots\times1=\frac{1}{\sqrt{\pi}}2^{(n+1)/2}\Gamma\left(\tfrac{n}{2}+1\right), && n\text{ odd}\\ n!!&=n\times(n-2)\times(n-4)\times\cdots\times2=n2^{(n-2)/2}\Gamma\left(\tfrac{n}{2}\right), && n\text{ even}\end{aligned}, \tag{22}$$

where $\Gamma(\cdot)$ is the Gamma function [6]. The reciprocal of the Taylor series is given as

$$g(s)=\frac{1}{f(s)}=\left(1+\sum_{n=2}^{\infty}b_n s^n\right)^{-1}=1-\sum_{n=2}^{\infty}c_n s^n \tag{23}$$

where the relationship between the sets $\{b_n\}$ and $\{c_n\}$ can be determined by evaluating

$$-c_n=\frac{1}{n!}\frac{\partial^n}{ds^n}\left(\frac{1}{f(s)}\right)\Bigg|_{s=0}. \tag{24}$$

Substituting (23) into (20) results in

$$
\begin{aligned}
I_2 &= 2\alpha^2 \int_{2\sqrt{\rho}}^{v'(x_0')/\alpha} \frac{1}{2\sigma}\left(1-\sum_{n=2}^{\infty} c_n s^n\right) d\sigma \\
&\equiv \alpha^2\left[\ln\left(\frac{v'(x_0')/\alpha}{2\sqrt{\rho}}\right) - \frac{1}{2}\int_0^1 \sum_{n=2}^{\infty} c_n s^{n-1} ds\right] \\
&= \alpha^2\left[\ln\left(\frac{v'(x_0')/\alpha}{2\sqrt{\rho}}\right) - \frac{1}{2}\sum_{n=2}^{\infty}\frac{c_n}{n}\right] \\
&= \alpha^2\left[\ln\left(\frac{v'(x_0')/\alpha}{2\sqrt{\rho}}\right) - \frac{1}{2}E\right]
\end{aligned}
\tag{25}
$$

The results presented below will depend upon E, which has been evaluated over the first several terms (using *Mathematica v2.0*) and has an approximate value of 0.1120. Substitution of (19) and (25) into (18) yields

$$
X = \frac{1}{2\pi^2}\left[\frac{1}{a}\ln\left(\frac{1+x_0/a}{1+x_0/a}\right) + \alpha^2\pi + \alpha^2\ln\left(\frac{\sqrt{x_0'}}{2\sqrt{\rho}}\right) - \frac{\alpha^2}{2}E\right] \tag{26}
$$

where the approximation $v'(x_0') \equiv \alpha\sqrt{x_0'}$ (applicable for $\rho << x_0'$) has been used. Either x_0 or x_0' in (26) can be eliminated using the relation in (16).

V. Selection of the normalizing parameter and transition point

As discussed above, the conditions $(a-x_0)/a \ll 1$, $\rho/(a-x_0) \ll 1$, and $\rho/x_0' \ll 1$ must be met for the approximations to be appropriate. As a preliminary step, we choose

$$\begin{aligned} a - x_0 &= \beta\rho \\ x_0' &= (\beta - 2)\rho \end{aligned} \tag{27}$$

The value of x_0' is chosen as in (27) to match the physical transition locations in the two geometries that are not exactly the same width. At the transition location, the complex potentials W and W', as well as the current distributions given by h_W^{-1} and $h_{W'}^{-1}$, must match to first order. Given the above constraints, the potentials and current match when

$$\alpha = \frac{\cos^{-1}(1-\beta\rho/a)}{\sqrt{\beta\rho}(1-1/\beta)}. \tag{28}$$

Substitution of (27) and (28) into (26) gives a result for X that depends only on choice of β.

A measure of the skin-loss efficiency of a current carrying conductor is given by the ratio of the actual circumference to the effective circumference (X^{-1}) [3]. The efficiency is defined in [3] as

$$\nu = [X\ell]^{-1}, \tag{29}$$

where ℓ is the circumference of the electrode. The value of ν is plotted as a function of β for various rollup sizes ρ/a in fig. 5. As predicted above, for sufficiently small ρ/a the transformations can be patched together over a large range of β. The appropriate value of β will be chosen where

$$\frac{\partial \nu}{\partial \beta} = 0. \tag{30}$$

Equation 30 was solved numerically for several values of ρ/a, and the resulting values of β are plotted as a function of rollup size in fig. 6. This data appears linear on a log-log plot, and using a least squares fit, the functional dependence

$$\beta_{fit} = 3.63(\rho/a)^{-0.50} \tag{31}$$

is obtained. Using the fitted form for β in (26) results in the curve for v as a function of ρ/a that is plotted in fig. 7.

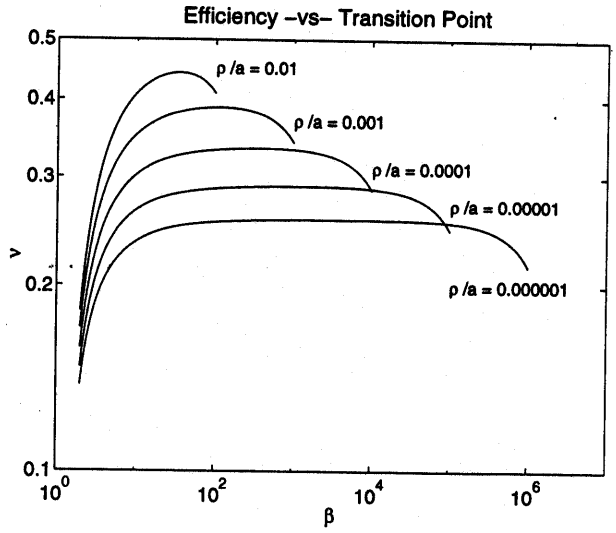

Figure 5: The skin-loss efficiency as a function of transition point x_0 for various rollup sizes.

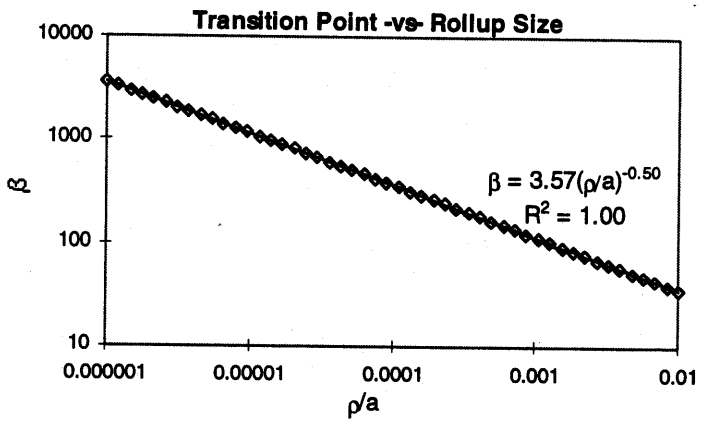

Figure 6: The fitted transition point (β_{fit}) as a function of rollup size. The fitted point is the location at which the rate of change of the efficiency in figure 5 is zero.

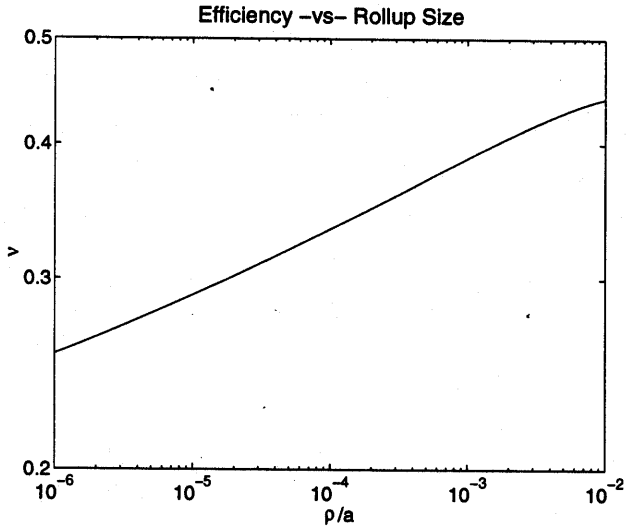

Figure 7: Skin-loss efficiency as a function of rollup size

VI. Conclusions

Previous work has indicated both analytically [3] and numerically [4] that the presence of sharp edges can degrade the rise-time of ultra-wideband pulses propagating on TEM transmission lines. Many UWB applications, such as launching transient signals via a TEM horn, necessarily involve propagating fast-rising pulses down TEM transmission lines with one or more sharp edges [8]. In these cases, methods may be developed to limit skin losses, which degrade the risetime. The concept of a high-voltage rollup has been employed to prevent electrical breakdown near sharp edges, and in this investigation, high-voltage rollups have been shown to also limit skin loss effects that result in risetime degradation.

REFERENCES

1. R. L. Wigington and N. S. Nahman, "Transient Analysis of Coaxial Cables Considering Skin Effects" *Proc. IRE,* pp. 166-174 (1957)

2. N. S. Nahman, "A Discussion of the Transient Analysis of Coaxial Cables Considering High-Frequency Losses" *IRE Trans. Circuit Theory* pp. 144-152 (1962)

3. C. E. Baum and J. S. Tyo, "Transient Skin Effects in Cables" *Measurement Notes*, Note 47, July 1996

4. C. J. Buchenauer, J. S. Tyo, and J. S. H. Schoenberg "Antennas And Electric Field Sensors For Ultra Wideband Transient Measurements: Applications And Methods" Ultra Wideband, Short-Pulse Electromagnetics III (Plenum Press, New York, In Publication)

5. D. V. Giri and C. E. Baum, "Equivalent displacement for a high-voltage rollup on the edge of a conducting sheet" Sensor and Simulation Notes, Note 294 (1986)

6. M. Abromowitz and I. A. Stegun *Handbook of Mathematical Functions* (Dover, New York, 1965)

7. D. Zwillenger (Ed.) *Standard Mathematical Tables and Formulae, 30th Edition* (CRC Press, Boca Raton, FL, 1996)

8. C. E. Baum, "Radiation of Impulse-Like Transient Fields" *Sensor and Simulation Notes* Note 321, (1989)